High spin states in ^{156}Yb ($N=86$)

C. J. Lister, D. Horn, C. Baktash, E. der Mateosian, O. C. Kistner, and A. W. Sunyar
Brookhaven National Laboratory, Upton, New York 11973
(Received 24 October 1980)

Yrast states in ^{156}Yb have been identified to spin and parity $J^\pi = 25^-$ at 7405 keV using the ^{144}Sm(^{16}O,4n)^{156}Yb (E = 70–120 MeV) and ^{113}In(^{46}Ti,$p2n$)^{156}Yb (E = 190–210 MeV) reactions together with standard γ-ray spectroscopic techniques. Evidence was found for additional transitions extending to J-30 at 9464 keV. One isomeric state was observed with $J^\pi = 11^-$ at E_x = 3028 keV, having $T_{1/2} = 6.0\pm0.5$ ns. The structure of this nucleus is compared with that of other N = 86 isotones. It appears that most of the features can be described in terms of relatively simple shell model configurations in a nearly spherical ($|\beta| \lesssim 0.1$) potential.

NUCLEAR REACTIONS ^{144}Sm(^{16}O, 4n)^{156}Yb E =70–120 MeV; ^{113}In(^{46}Ti, $p2n$) ^{156}Yb E =190–210 MeV. Measured E_γ, I_γ, linear polarizations, γ-γ, γ-x-ray, γ-charged particle coincidences, pulsed beam lifetimes. Deduced level energies, branching ratios, spin and parity assignments, multipole mixing ratios, electromagnetic transition strengths. Ge(Li) detectors. Enriched targets. Comparison with systematic trends.

I. INTRODUCTION

The suggestion by Bohr and Mottelson[1] that at very high spin nuclei may attain oblate shapes and exhibit isomerism has stimulated a host of experimental and theoretical studies aimed at observing such phenomena and understanding the isomeric structure in detail. While an island of isomers was found[2] with $A \sim 150$, incontestable evidence for this type of oblate deformation remains elusive. However, a wealth of interesting nuclear structure features has been uncovered, especially among those nuclei with a few valence nucleons in excess of the effective double shell closure at $Z = 64$, $N = 82$.[3] The isomers appear to be simple shell-model ones involving low energy transitions with approximately single-particle rate electromagnetic decays. Important nuclear structure information has emerged through measurements of their electromagnetic moments.[4,5] The existence of these isomers has also made possible the study of very high spin states and the continuum via prompt-delayed γ-ray coincidence techniques.[6,7]

The investigation of discrete states to excitation energies as high as $E_x \sim 12$ MeV and spin $J > 37\hbar$ has been possible in several nuclei because of an unusually high population of yrast states at angular momentum $J > 30\hbar$. The mechanism for this process is not clear at present, but is the subject of several studies.[7,8] In particular, the $N = 86$ isotones ^{150}Gd, ^{152}Dy, and ^{154}Er (Refs. 9, 6, and 10, respectively) have been examined in detail. Several features, even at high excitation and spin, appear to arise from relatively simple few-particle shell model configurations in a nearly spherical ($|\beta| \leq 0.1$) potential.[11] In order to trace these features across a wider range of isotones the $Z = 70$, $N = 86$ nucleus ^{156}Yb has been studied and is discussed in this paper. No excited states in ^{156}Yb were known at the onset of this work, so a preliminary identification of the γ rays from this nucleus was needed and is described in Sec. II. Section III presents the results of these experiments. The structure of ^{156}Yb is discussed and compared with $N = 86$ systematics in Sec. IV.

II. EXPERIMENTAL METHOD

Since excited states of ^{156}Yb had not been previously reported, an investigation of all γ rays produced from the ^{16}O + ^{144}Sm reaction was necessary to establish those transitions which originated from the decay of levels in ^{156}Yb. A variety of techniques were used, as calculations using the evaporation codes ALICE (Ref. 12) and CASCADE (Ref. 13) indicated that neutron, proton, and alpha particle emission were all significant in deexciting the compound nucleus. A measurement of the relative γ-ray yield as a function of energy was made by bombarding a ^{208}Pb backed, 3.5 mg/cm^2 ^{144}Sm target (enriched to >96%) by 80–120 MeV ^{16}O beams. This allowed γ rays to be grouped into categories associated with 2, 3, or 4 particle evaporation. Further specification was accomplished by detecting alpha particles and protons in coincidence with γ rays. The charged particles were detected by a 978 μm thick fully depleted Si surface barrier detector which was shielded from electrons and scattered beam particles by a Ni foil. X rays were detected with Ge(Li) detectors and measured in coincidence with gamma rays to provide conclusive Z assignments. The combination of these techniques allowed the assignment of transitions to the nuclei ^{156,7}Yb and ^{156,7}Tm, all of which were previously unknown. A full analysis of the data on the odd A nuclei ^{157}Yb and ^{157}Tm is in progress and will be presented separately. The optimum ^{16}O beam energy for producing ^{156}Yb relative to other nuclei was found to be 107 MeV.

States in ^{156}Yb were also populated using the ^{113}In(^{46}Ti, $p2n$) ^{156}Yb reaction [$E(^{46}$Ti$)=150-210$ MeV] in order to confirm the assignments. An attempt was made to observe the β^+ decay of ^{156}Lu populated via the ^{113}In(^{46}Ti, $3n$)^{156}Lu reaction by interrupting the beam with a mechanical chopper. No γ lines associated with ^{156}Yb were observed in the "beam-off" periods, presumably because the decay is dominated by an α-decay branch from both ^{156}Lu ground and isomeric states.

Gamma-gamma coincidence data, collected with both continuous and pulsed beams, were used to construct the decay schemes of the new nuclei produced. These data were taken using the ^{16}O $+^{144}$Sm reaction at 107 MeV. The pulsed beam studies were made with bursts of 6 ns full width at half maximum (FWHM) repeated every 500 ns. Multiparameter data were sorted online and stored on tape. Subsequent analysis revealed the location of previously unreported isomeric states in several nuclei.

Angular distribution measurements were made at 105 and 113 MeV at eight angles in the range 70–160° with respect to the beam direction. A separate experiment was required to measure the angular distribution of the 72 keV line in ^{156}Yb, as intense x rays from the Pb target backings and beam stops totally obscured this transition in normal singles spectra. For this measurement a target of 2.4 mg/cm^2 ^{144}Sm was used, backed by a 3.5 mg/cm^2 ^{120}Sn foil. With this target backing neither x rays nor γ rays from the ^{16}O$+^{120}$Sn interaction were found near 70 keV. To improve the resolution for low energy transitions an intrinsic germanium planar detector 10 mm thickness and 650 eV resolution at 122 keV was used in place of the 18–22% efficiency true-coaxial Ge(Li) detectors (with resolutions <2.0 keV at 1.33 MeV) used in all other parts of these studies.

Gamma-ray linear polarization measurements were made using a 2-Ge(Li) Compton polarimeter which has been described previously.[14] This apparatus was calibrated with γ rays from the ^{150}Nd(^{13}C, $5n$)^{158}Dy reaction at 75 MeV, which had been studied previously in this laboratory.[15] The strongly populated ground state band allowed calibration through the study of stretched $E2$ decays in the energy range 218–678 keV. The sign convention used in data analysis was that of Fagg and Hanna.[27] In this range the sensitivity of the apparatus, Q, was found to be a constant fraction of the sensitivity predicted by the Klein-Nishina formula derived for point detectors in this geometry. The sensitivity was

$$Q_{\text{expt}}=0.57\pm0.07\ Q_{\text{KN}}\ .$$

Final analysis involved the elimination of multiply scattered and escape events by ensuring that the coincident gamma ray energies satisfied the kinematical constraints for single Compton scattering in the experimental geometry.

III. RESULTS

A selection of yield curves for γ rays identified in this experiment is shown in Fig. 1. Transitions in ^{156,7}Yb, ^{156,7}Tm, and ^{154,5}Er are displayed and compared with the predictions of the evaporation code CASCADE.[13] The initial use of this program in an "all defaults" mode resulted in a mean difference in peak yield between experiment and calculation of more than 10 MeV. However, an adjustment of the calculated Coulomb barrier to reproduce recent experimental measurements[16] and the use of empirical[17] rather than liquid drop masses reduced the mean difference between calculation and experiment to less than 7 MeV. For clarity of comparison the experimental and calculated yield curves in Fig. 1 are normalized at the peak of the $3n$ evaporation channel at 92 MeV. The strongest lines associated with these nuclei are also given in Table I.

A strong cascade of 13 transitions was observed in ^{156}Yb, together with several weaker γ rays. Figure 2 shows these transitions in a spectrum containing the sum of selected γ-γ coincidence projections from windows set on γ rays found only in this nucleus. Establishing the correct sequence of levels in this cascade presented some difficulty, particularly near $E_x=6.2$ MeV where similar intensities populating and depopulating states indicated very little sidefeeding. However, the final decay scheme deduced from cross bombardments, relative yield curves, and singles and coincidence intensities is shown in Fig. 3.

The pulsed beam data revealed one isomeric state in ^{156}Yb at 3028 keV. High lying transitions were found to occur promptly with respect to the beam bursts indicating half-lives of less than 3 ns, while the γ-beam pulse time distributions of low-lying levels all exhibited a half-life component of

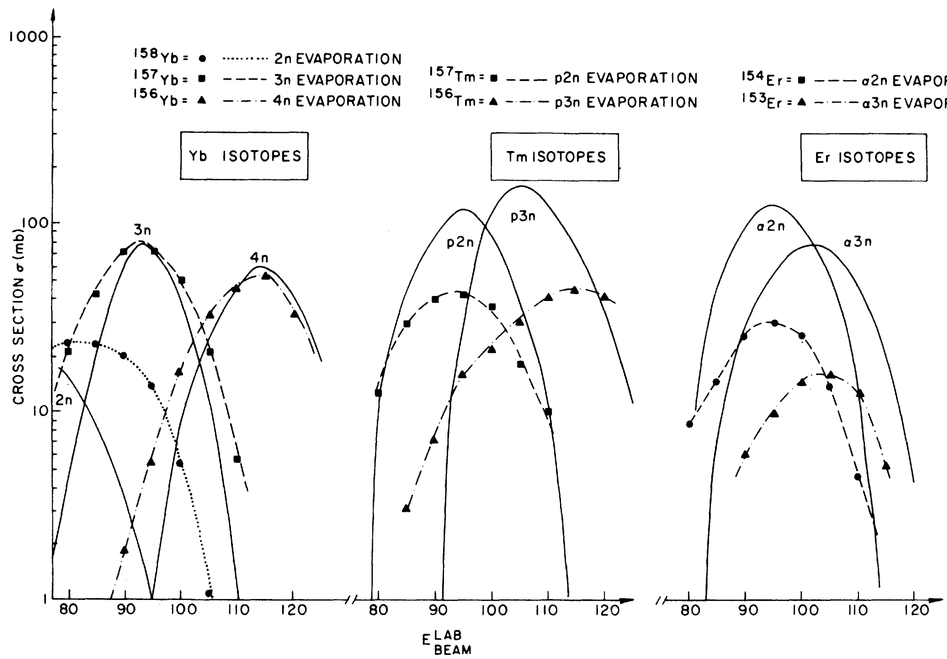

FIG. 1. The relative γ-ray yields from *xn*, *pxn*, and *αxn* exit channels following the $^{16}O + ^{144}Sm$ compound nuclear reaction at beam energies $E = 80-120$ MeV. Also shown are the cross sections calculated using the evaporation code CASCADE. The experimental yields are normalized to the calculated 3*n* cross section at 92 MeV. An energy offset is made to the calculation, which is discussed in the text.

$T_{1/2} = 6.0 \pm 0.5$ ns. Figure 4 illustrates the time spectra associated with both prompt and isomeric decays.

Gamma ray intensities from the angular distribution data were fitted to an expansion of even Legendre polynomials to fourth order. The results from these fits are shown in Table II, which is a compilation of all measurements made on ^{156}Yb in this work. The members of the strong cascades from 7405 to 3026 keV ($J^\pi = 25^- - 11^-$) and from 2956 keV ($J^\pi = 10^+$) to ground all appear to be $E2$ transitions, with positive a_2 and smaller negative a_4 polynomial coefficients and positive polarizations. The nuclear alignment deduced from these cascades increases smoothly with excitation energy, varying from 35% of maximum alignment for the $2^+ \rightarrow 0^+$ transition to nearly full alignment for decays above 7 MeV. The assign-

TABLE I. A list of characteristic gamma rays for the nuclei observed in this work. The lines listed are chosen as they occur dominantly in just one nucleus, although they may not be the strongest. The relative intensities are taken from $^{16}O + ^{144}Sm$ data at the peak yield energy for that nucleus. Gamma ray energies are accurate to ±0.1 keV, relative intensities to ±5%.

Nucleus	Evaporation from ^{160}Yb CN	Bombarding energy for in $^{16}O + ^{144}Sm$ (MeV)	E_γ (I_{rel}) [a]
^{158}Yb	2*n*	80	357.7(100), 476.4(100)
^{157}Yb	3*n*	93	494.5(100), 491.0(83)
^{156}Yb	4*n*	114	607.4(100), 500.0(24), 375.6(16)
^{157}Tm	*p*2*n*	94	393.2(100), 520.8(97), 732.5(73)
^{156}Tm	*p*3*n*	115	567.9(100), 595.0(70), 479.3(23)
^{155}Er	*αn*	<80	531.6(100), 475.8(94)
^{154}Er	*α*2*n*	95	560.4(100), 668.8(43), 318.3(30)
^{153}Er	*α*3*n*	105	299.4(100), 811.8(95), 712.1(80)
^{152}Er	*α*4*n*	>120	422.6(100), 280.0(90)

[a] The relative intensities are normalized to the strongest clean line in each nucleus.

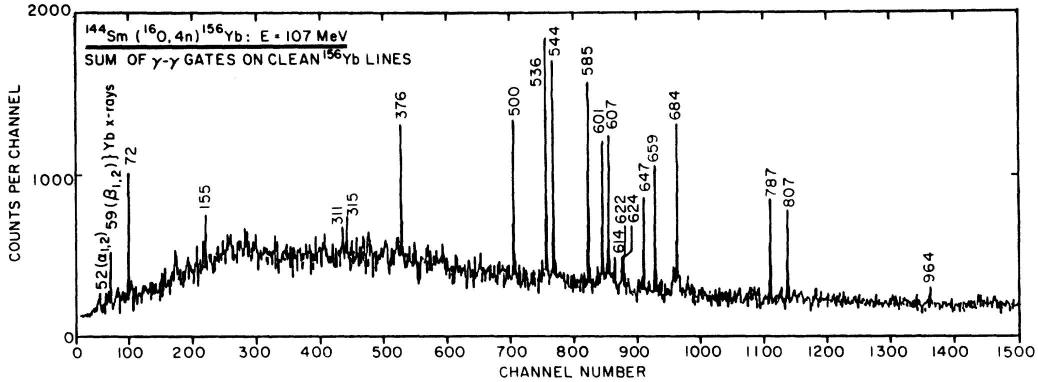

FIG. 2. A representative spectrum of γ rays from ^{156}Yb formed from the γ-γ coincidence data. The dispersion is 0.71 keV per channel.

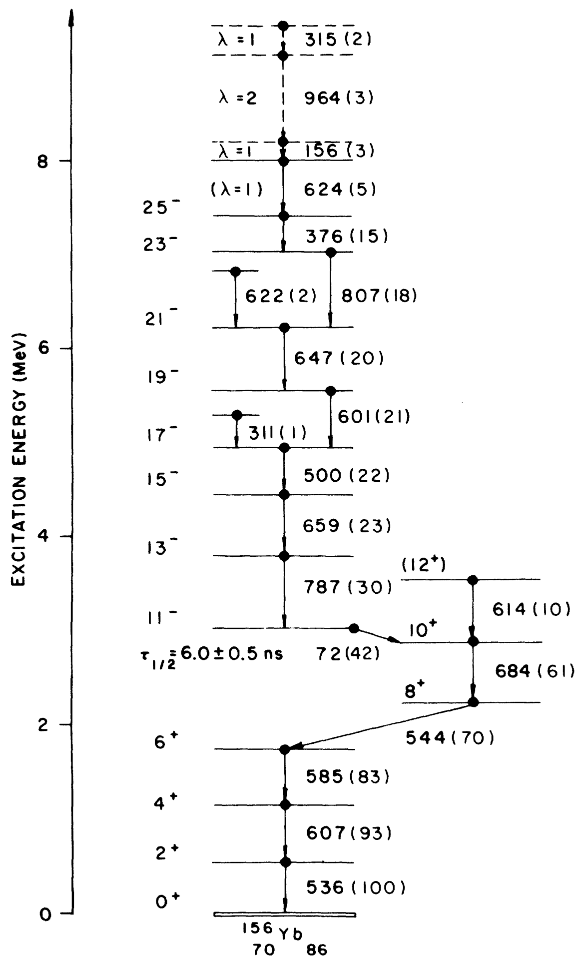

FIG. 3. The decay scheme of ^{156}Yb. Transition intensities are corrected for internal conversion. The error on γ-ray intensities is less than 5% with the exception of that of the highly converted 72 keV line which is ± 20%. Some doubt lies over the relative ordering of the 647 and 807 keV members of the main cascade which is discussed in the text.

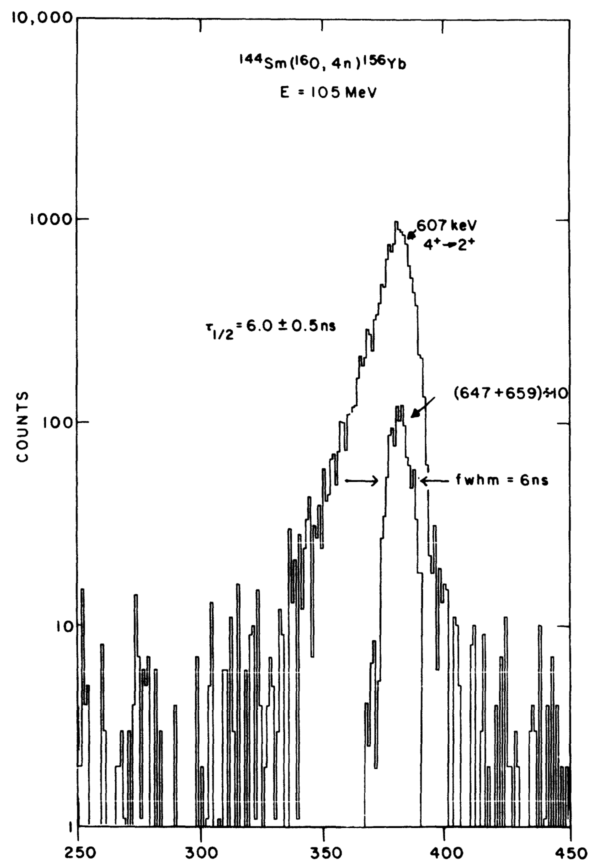

FIG. 4. A sample of the pulsed beam data to illustrate the decay of the $J = 11^-$ isomer at 3028 keV. The spectrum shown is a time distribution of γ rays detected in a Ge(Li) detector following a beam burst. Typical prompt and delayed distributions are shown.

TABLE II. A compilation of properties of γ ray transition in ^{156}Yb. Included are initial and final energy levels, γ-ray energies, angular distribution coefficients, linear polarizations, and multipolairty assignments. Transitions marked (a) in the polarization column were members of complicated multiplets in the singles spectra preventing any measurement of the γ-rays properties; levels marked (w) were too weak to allow extraction of a reliable polarization.

E_i	E_f	E_γ	a_2	a_4	$P_z(90)$	$J_i^\pi \to J_f^\pi$
536	0	536.4 ± 0.1	+0.24(2)	−0.12(3)	0.44(2)	$2^+ - 0^+$
1144	536	607.3 ± 0.2	+0.23(3)	−0.11(4)	0.58(2)	$4^+ - 2^+$
1728	1144	584.8 ± 0.1	+0.23(1)	−0.12(2)	0.40(5)	$6^+ - 4^+$
2273	1728	544.1 ± 0.1	+0.28(2)	−0.13(2)	0.57(15)	$8^+ - 6^+$
2956	2273	683.9 ± 0.1	+0.27(3)	−0.10(5)	(+)	$10^+ - 8^+$
3028	2956	71.8 ± 0.1	−0.31(5)	+0.09(7)		$11^- - 10^+$
3571	2956	614.5 ± 0.2			(a)	$(12^+) - 10^+$
3816	3028	787.5 ± 0.1	−0.29(2)	−0.07(3)	0.69(4)	$13^- - 11^-$
4475	3816	659.3 ± 0.1	+0.27(3)	−0.06(5)	0.78(5)	$15^- - 13^-$
4975	4475	500.0 ± 0.1	+0.34(3)	−0.09(4)	0.79(9)	$17^- - 15^-$
5285	4975	310.9 ± 0.3	+0.24(5)	−0.02(3)	(+)	$\lambda = 2$
5576	4975	600.6 ± 0.1	+0.26(2)	−0.04(3)	0.50(4)	$19^- - 17^-$
6223	5576	646.9 ± 0.1	+0.30(4)	−0.03(2)	1.00(20)	$21^- - 19^-$
6845	6223	622.1 ± 0.2			(a)	
7029	6223	806.7 ± 0.1	+0.38(6)	−0.04(9)	0.62(7)	$23^- - 21^-$
7405	7029	375.7 ± 0.1	+0.44(7)	−0.16(12)	0.44(11)	$25^- - 23^-$
8029	7405	624.2 ± 0.2			(a)	$\lambda = 1$
8185	8029	155.7 ± 0.3	−0.31(12)	+0.11(16)	(w)	$\lambda = 1$
9149	8185	964.4 ± 0.5	+0.41(12)	−0.10(20)	(+)	$\lambda = 2$
9464	9149	315.3 ± 0.3	−0.32(18)	−0.03(2)	(w)	$\lambda = 1$

ments of spin and parity from the ground state to the $J^\pi = 10^+$ state at 2956 keV were straightforward, but all higher assignments depended on the multipolarity of the 71.8 keV transition from the 3028 keV state. The angular distribution of the γ-ray part of this decay was measured and indicated a $\Delta J = 1$ decay with a mixing ratio $\delta \approx 0$. The average alignment deduced from the $E2$ decays above (787 keV) and below (684 keV) this transition was $\sigma/J = 0.25$. This value was taken to extract[18] a mixing ratio of $\delta = -0.07 \pm 0.04$. In addition, the intensity of the unconverted part of the decay was measured relative to other ^{156}Yb lines. The total intensity of this decay must be greater than that of the 787 keV line, while the sum of this and the intensity of the (12^+) 615 keV decay must be less than the 684 keV intensity. These limitations bracket the total conversion coefficient as $1.28 \leq \alpha_{tot} \leq 3.98$. Using the tables of conversion coefficients calculated by Rösel *et al.*[19] one calculates that this restriction limits the multipolarity of this decay to an $E1/M2$ mixture with $0.06 \leq \delta \leq 0.18$. These estimates of mixing ratio agree rather well if the intensity of the 71.8 keV decay is slightly larger than that of the 787 keV transition and correspond to electromagnetic transition strengths of $B(E1) = 11 \pm 1$ mW.u. and $B(M2) = 4 \pm ^6_3$ W.u. These measurements fix the spin and parity of the isomer as $J^\pi = 11^-$.

Above the isomer a series of negative parity states was found which decay through a cascade of $E2$ transitions. The highest state in this sequence at 7405 keV has $J^\pi = 25^-$. Using the O + Sm reaction at 107 MeV the decay from this state had 15% of the ^{156}Yb $2^+ \to 0^+$ strength. However, above this point the intensity of population of levels decreased sharply and all higher assignments must be considered tentative. A 624 keV γ ray was found in coincidence with all lower lines, but was contaminated in singles data by the strong $6^+ \to 4^+$ 625 keV decay in ^{154}Er. A tentative dipole assignment was made on the basis of directional correlation ratios measured in the γ-γ coincidence study. Higher lying transitions of 156, 315, and 964 keV energy were clear in coincidence windows set on the upper members of the main cascade. They were individually too weak to be conclusively shown to be in mutual coincidence, although their relative intensities support this suggestion. Sidebranches with energies of 614, 311, and 622 keV were observed joining the yrast sequence at spin $J = 10$, 17^-, and 21^- but these transitions were also too weak to investigate thoroughly.

IV. DISCUSSION

No shell model calculations have been published specifically for ^{156}Yb, and the quality of agreement between calculation and experiment is poor for those $N=86$ isotones which have been studied in detail.[20] These calculations use a deformed potential (of harmonic oscillator or Woods-Saxon type) with a deformation parameter which can be varied to minimize the energy of each configuration. The residual interaction of nucleons in the same shell is neglected, and probably because of this the calculations reproduce only the gross features of the level schemes and provide some indications as to which configurations are yrast. A fruitful empirical approach to understanding the level structure in this region has been taken by Kleinheinz *et al.*[21] who used one- and two-particle spectra from nuclei adjacent to ^{146}Gd ($Z=64$, $N=82$) to construct the level schemes of other nuclei in this area and to deduce the dominant components in level wave functions. While this approach loses validity as one moves away from the shell closure, it has provided useful guidelines for understanding the $N=86$ systematics, especially among the higher spin states where relatively few configurations can contribute to the structure of each level.

The simplicity of the decay scheme of ^{156}Yb, when compared to the other even $N=86$ isotones, is striking. Almost all the states populated by the heavy ion reactions used in this work decay through a single series of levels. This is manifestly different from neighboring isotones ^{150}Gd, ^{152}Dy, and ^{154}Er in which both positive and negative parity high spin sequences are well developed, as are low spin, low excitation negative parity states. Two underlying features which vary smoothly with Z across the $N=86$ isotones may be identified as the cause of this apparently sudden change in level schemes. Firstly, proton configurations, especially the highly aligned ones such as $(h_{11/2})^n_{J=8,10}$, are found at highest excitation in the semimagic nucleus ^{150}Gd and lie regularly lower with increasing Z in ^{152}Dy and ^{154}Er. In contrast, low spin negative parity states are found at lowest excitation in ^{150}Gd and at regularly higher excitation with increasing Z. The combination of these two effects gives ^{156}Yb a very clear-cut yrast sequence which carries almost all of the decay intensity. The cause and influence of these trends is discussed in more detail in the following paragraphs.

In ^{156}Yb, as in all the $N=86$ isotones, the low-lying positive parity levels $J=2^+$, 4^+, and 6^+ are rather evenly spaced with gamma transitions $E\approx 600$ keV. Many configurations may be admixed into these states and their wave functions are complex mixtures of neutron $(f_{7/2}h_{9/2}i_{13/2})^4$ and proton $(h_{11/2})^6$ configurations. Although ^{154}Yb, with the $N=84$, $(h_{11/2})^6$ spectrum, is not known, one may surmise from the $(h_{11/2})^4$ and $(h_{11/2})^2$ spectra of ^{152}Er and ^{150}Dy (Refs. 22 and 23, respectively) that proton configurations contribute only small amplitudes to low spin states, but probably contribute significant admixtures for $J\gtrsim 8$. The compression of the low spin ($J=2^+$ -10^+) positive parity spectrum across the $N=86$ isotones may be attributed to an increase of proton admixture with the increasing number of valence protons.

The fact that low-lying negative parity states built on octupole core vibrations are not seen in ^{156}Yb may be attributed to the blocking of shell model orbits above the $Z=64$, $N=82$ effective shell closure. In ^{146}Gd, the closed shell nucleus, the $h_{11/2}$ proton and $f_{7/2}$, $h_{9/2}$, and $i_{13/2}$ neutron orbits are vacant and a very collective octupole phonon state [$B(E3)=37\pm 4$ W.u.] is found[28] as the first excited level. The addition of four neutrons to form ^{150}Gd blocks some of the 1p-1h neutron excitation and hence reduces collectivity, but a $J^\pi=3^-$ state is still clearly developed. The measurement of nuclear g factors in ^{146,147}Gd by Faestermann *et al.*[24] indicate that this state is dominated by a $(h_{11/2}d_{5/2}^{-1})$ 1p-1h configuration. However, in ^{152}Dy, ^{154}Er, and ^{156}Yb the $h_{11/2}$ proton orbit becomes successively fuller and particle-hole excitations are more completely blocked. Consequently, the 3^- state (and configurations built on it) are forced to lie high above adjacent yrast levels and cease to be seen. In ^{152}Dy $J=5^-, 7^-, 9^-$ states are seen; in ^{154}Er only $J=7^-$ and 9^- appear; while in ^{156}Yb, none of these levels are found. This is probably because the 9^- state lies above the 11^- isomer and so is not in the yrast sequence.

In contrast to the low spin negative parity states, a $J^\pi=11^-$ level is seen in all of the $N=86$ isotones which have been studied in detail. The excitation energy of this state is almost constant in these nuclei and so presumably arises from a neutron configuration. The lowest energy state that may be formed this way is the aligned $\nu(h_{9/2}\otimes i_{13/2})_{11^-}$ configuration. The separate description of low and high spin negative parity states was originally put forward by Vogel[25] and appears to be supported by these systematic trends. The $J^\pi=11^-$ state is isomeric in ^{152}Dy($t_{1/2}=4$ ns),[26] ^{154}Er($t_{1/2}=40$ ns),[10] and ^{156}Yb($t_{1/2}=6$ ns).

Built on the $J^\pi=11^-$ isomer is a sequence of levels connected by $E2$ transitions which extends to $J^\pi=25^-$. The decreasing energy spacing of the first three states is reminiscent of a j^2 multiplet and suggests further neutron alignment which culminates in the $[(f_{7/2}{}^2)_{6^+}\otimes(h_{9/2}i_{13/2})_{11^-}]_{17^-}$ configuration. However, the ratio of level spacings $E(17^- - 15^-)/E(17^- - 11^-)$ is about twice that which one calculates for an $f_{7/2}^2$ multiplet using a δ interaction, or which is experimentally observed in $f_{7/2}^2$ spectra. Such a change from the characteristic pattern may be an indication these configurations are not pure.

Above the 17^- state at 4975 keV, which involves nearly full neutron alignment, one may expect proton-excited configuration to play a more significant role. The 19^- states in ^{150}Gd and ^{152}Dy clearly have a very different structure from that of the 17^- levels as they decay only to the 18^+ states with no $19^- \to 17^-$ branches observed. In contrast, in ^{154}Er and ^{156}Yb, the $19^- \to 17^-$ transition is the only one observed with no detectable branches to positive parity states. This change may be attributed to the decrease of excitation energy of proton configurations with increasing Z, which lowers the energy of the $J^\pi = 19^-$ state to a point where decay to high spin positive parity states is energetically unfavorable and, at the same time, leads to the 17^- states having larger proton amplitudes.

It has been pointed out by Baktash *et al.*[11] that built on the $J^\pi = 19^-$ state in ^{154}Er (and $J^\pi = 21^-$ in ^{150}Gd and ^{152}Dy) lies a sequence of states which correspond very closely to the $J^\pi = 0^+,\ 2^+,\ 4^+,\ 6^+$ series in their respective $N = 84$ isotopes. This observation was attributed to the near maximum alignment of the valence particles culminating in $[\pi(h^n_{11/2})_{8^+,10^+} \otimes \nu(h_{9/2}i_{13/2})_{11^-}(f_{7/2}{}^2)_{6^+}]_{25^-,27^-}$. The data for ^{156}Yb partially support this explanation. Feeding the 19^- state lies a sequence of gamma rays with transition energies of 807, 647, and 376 keV. These transition energies are very similar to those found in the $f_{7/2}^2$ multiplets seen in the $N = 84$ isotopes.[22,23] However, to provide the necessary intensity balance to confirm this sequence, a 7029 to 6845 keV transition of 184 keV in parallel with the 807 keV decay would be required of intensity 1 unit relative to the intensity $(2^+ \to 0^+) = 100$ transition. In ^{154}Er the corresponding decay has been found to have an $M1$ multipolarity (Ref. 29) which reduces the gamma intensity due to internal conversion. No evidence could be found for such a decay in this work, neither in singles nor in coincidence data, although the transition would be at the limit of sensitivity. Consequently the unusual level order displayed in Fig. 3 reflects the experimentally observed intensities.

The systematics of the $N = 86$ even-even nuclei (for example, manifestation of level spacings typical of j^2 configurations in a nearly spherical potential) suggest that the quadrupole deformation is not very large (Ref. 11). This would be in contrast with recent measurements of some quadrupole moments in ^{146,147}Gd by Haüsser *et al.*[5] who have concluded that (oblate) deformation increases with spin and becomes as large as $\beta \approx -0.2$ for the $J = \frac{49}{2}$ isomeric state in ^{147}Gd. However, a recent calculation by Dossing *et al.*[20] shows that although quadrupole deformation may reach values as high as -0.2 for the high spin states in the $N \approx 82$ nuclei, it generally decreases with increasing neutron number, and ranges around $|\beta| \approx 0.1$ for the $N = 86$ nuclei. In the $N \approx 82$ region, Kleinheinz *et al.* have successfully interpreted the low-lying yrast and near-yrast states in terms of simple shell model configurations in a spherical basis (see, e.g., Ref. 3). The measured and calculated deformation for some of these states range around 0.05. It therefore seems that despite the presence of some deformation in the $N = 86$ nuclei, similar shell model calculations may provide a useful insight into the structure of the yrast high spin states in these nuclei, and in particular identify the main component in their wave functions.

Above $J^\pi = 25^-$ the observed population of states falls rapidly. A similar, although less marked decrease is also observed in ^{154}Er. Candidates for levels with spins up to $J \sim 30$ have been found in this work but their population was too weak to extract structural information. Presumably the production of ^{156}Yb with reactions induced by heavier ions would increase the population of high spin states. However, competition from other reaction channels makes the γ-ray spectra very complex and presents the main barrier to learning more about the states at higher excitation.

V. CONCLUSION

The principal γ decays in ^{156,7}Yb and ^{156,7}Tm have been identified. High spin states have been observed in ^{156}Yb to spins near $J = 30$. Many systematic trends observed in other $N = 86$ isotones were followed here, and are explicable in terms of simple shell-model configurations in a nearly-spherical ($|\beta| \lesssim 0.1$) potential. The interpretation of these data, and those recently obtained for many other nuclei in this region would be greatly helped by conventional shell model calculations in a spherical basis. It is hoped that this work encourages progress in that direction.

ACKNOWLEDGMENTS

The authors would like to thank I. Feigenbaum for production of targets and the crew of the BNL Van de Graaff for efficient operation. This work was supported by the Division of Basic Energy Sciences, DOE, under Contract No. DE-AC02-76CH00016.

[1]A. Bohr and B. R. Mottelson, Phys. Scr. 10A, 13 (1974).

[2]J. Pedersen, B. B. Back, F. M. Bernthal, S. Bjørnholm, J. Borggreen, O. Christensen, F. Folkmann, B. Herskind, T. L. Khoo, M. Neiman, F. Pühlhofer, and G. Sletten, Phys. Rev. Lett. 39, 990 (1977).

[3]A review of many recent experiments may be found in Proceedings of the Symposium on High Spin Phenomena in Nuclei, Argonne, Illinois, edited by T. L. Khoo (ANL Report No. ANL-PHYS-79-4, 1979).

[4]O. Häusser, P. Taras, W. Trautmann, D. Ward, T. K. Alexander, H. R. Andrews, B. Haas, and D. Horn, Phys. Rev. Lett. 42, 1451 (1979).

[5]O. Häusser, H. E. Mahnke, J. F. Sharpey Schafer, M. L. Swanson, P. Taras, D. Ward, H. R. Andrews, and T. K. Alexander, Phys. Rev. Lett. 44, 132 (1980).

[6]T. L. Khoo, R. K. Smither, B. Haas, O. Häusser, H. R. Andrews, D. Horn, and D. Ward, Phys. Rev. Lett. 41, 1024 (1978).

[7]J. F. Sharpey Schafer, A. J. Ferguson, H. R. Andrews, O. Häusser, H-E. Mahnke, and D. Ward, contributions to the International Conference on Nuclear Behavior at High Angular Momentum, Strasbourg, France, 1980, p. 65.

[8]J. Borggreen *et al.*, Bull. Am. Phys. Soc. 25, 605 (1980).

[9]C. Baktash, E. der Mateosian, O. C. Kistner, A. W. Sunyar, D. Horn, and C. J. Lister, contributions to the International Conference on Band Structure and Nuclear Dynamics, Tulane, 1980; Bull. Am. Phys. Soc. 24, 828 (1979).

[10]C. Baktash, E. der Mateosian, O. C. Kistner, and A. W. Sunyar, Phys. Rev. Lett. 42, 637 (1979).

[11]C. Baktash, E. der Mateosian, O. C. Kistner, A. W. Sunyar, D. Horn, and C. J. Lister, Proceedings of the International Conference on Nuclear Physics, Berkeley, 1980 (LBL, to be published), Vol. I, p. 323.

[12]M. Blann and F. Plasil, USAEC Report No. C00-3494-10 (unpublished); M. Blann, Nucl. Phys. 80, 223 (1966).

[13]F. Pühlhoffer, Nucl. Phys. A280, 267 (1977).

[14]O. C. Kistner, A. W. Sunyar, and E. der Mateosian, Phys. Rev. C 17, 1417 (1978).

[15]P. Thieberger, A. W. Sunyar, P. C. Rogers, N. Lark, O. C. Kistner, E. der Mateosian, S. Cochavi, and E. H. Auerbach, Phys. Rev. Lett. 28, 972 (1972).

[16]R. G. Stokstad, Y. Eisen, S. Kaplanis, D. Pelte, U. Smilansky, and I. Tserruya, Phys. Rev. C 21, 2427 (1980).

[17]A. H. Wapstra and K. Bos, At. Nucl. Data Tables 19, 175 (1977).

[18]E. der Mateosian and A. W. Sunyar, At. Nucl. Data Tables 13, 407 (1974).

[19]F. Rösel, H. M. Fries, K. Alder, and H. C. Pauli, At. Nucl. Data Tables 21, 91 (1978).

[20]See, for example, A. Faessler and M. Ploszajczak, Z. Phys. A 295, 87 (1980) and references therein; T. Dossing, K. Neergard, and H. Sagawa, NBI Report No. 80-34.

[21]P. Kleinheinz, Proceedings of the Symposium on High Spin Phenomena in Nuclei, Argonne, Illinois, edited by T. L. Khoo (ANL Report No. ANL-PHYS-79-4, 1979), p. 125.

[22]D. Horn, G. R. Young, C. J. Lister, and C. Baktash, Phys. Rev. C 23, 1047 (1981).

[23]S. Lunardi, M. Ogawa, H. Bake, M. Piiparinen, Y. Nagai, and P. Kleinheinz, Proceedings of the Symposium on High Spin Phenomena in Nuclei, Argonne, Illinois, edited by T. L. Khoo (ANL Report No. ANL-PHYS-79-4, 1979), p. 403.

[24]T. Faestermann, H. Bohn, F. Feilitzsch, A. W. Sunyar, R. Broda, P. Kleinheinz, and M. Ogawa, Phys. Lett. 80B, 190 (1979).

[25]P. Vogel, Phys. Lett. 60B, 431 (1976).

[26]Y. Nagai, J. Styczen, M. Piiparinen, and P. Kleinheinz, Z. Phys. A 296, 91 (1980).

[27]L. W. Fagg and S. S. Hanna, Rev. Mod. Phys. 31, 711 (1959).

[28]P. Kleinheinz, R. Broda, P. J. Daly, S. Lunardi, and M. Ogawa, Z. Phys. A 290, 279 (1979).

[29]C. Baktash, E. der Mateosian, O. C. Kistner, A. W. Sunyar, C. J. Lister, and D. Horn (unpublished).